

# 1 Introducing a new rock abrasivity index using a scaled down disc cutter

2  
3 Maziar Moradi<sup>1</sup>, Mohammad Hossein Khosravi<sup>2\*</sup> and Jafar Khademi Hamidi<sup>3</sup>

4 1) Department of Civil and Environmental Engineering, University of Strathclyde, United  
5 Kingdom

6 2) Department of Mining Engineering, Faculty of Engineering, University of Birjand, Birjand,  
7 Iran, ORCID: 0000-0002-7600-5786

8 3) Mining Engineering Department, Faculty of Engineering, Tarbiat Modares University, Tehran,  
9 Iran, ORCID: 0000-0001-8820-3256

10 \*Corresponding author: Mohammad Hossein Khosravi ([mh.khosravi@birjand.ac.ir](mailto:mh.khosravi@birjand.ac.ir)),

## 11 12 **Abstract**

13 Rock abrasivity influences wear of cutting tools and consequently, performance of mechanized  
14 tunneling machines. Several methods have been proposed to evaluate rock abrasivity in recent  
15 decades, each one has its own advantages. In this paper, a new method is introduced to estimate  
16 wear of disc cutters based on rock cutting tests using scaled down discs (i.e. 54 and 72 mm  
17 diameter). The discs are made of H13 steel, which is a common steel type in producing real-scale  
18 discs, with hardness of 32 and 54 HRC. The small-scale linear rock cutting machine and a new  
19 abrasion test apparatus, namely University of Tehran abrasivity test machine, are utilized to  
20 perform the tests. Tip width of the worn discs is monitored and presented as the function of the  
21 accumulated test run to classify the rock abrasion. Abrasivity tests show that by increasing the  
22 UCS of the rock samples, wear rate is doubled gradually that reveals the sensitivity of the test  
23 procedure to the main parameters affecting the abrasivity of hard rocks. For the rocks with the  
24 highest UCS, the normal wear stops after performing 5 to 10 rounds of the tests, and then,  
25 deformation of the disc tip is detectable. Two abrasivity indices are defined based on the abrasivity  
26 tests results and their correlations with CAI and UCS are established. Comparison of the  
27 established correlations in this study with previous investigations demonstrates the sensitivity of  
28 the indices to the parameters affecting wear of the disc cutters and repeatability of the outputs  
29 obtained from abrasivity tests using scaled down discs. Findings of this study can be used to  
30 enhance the accuracy of rock abrasivity classifications.

31 **Keywords:** Mechanized tunneling, Rock cutting, Rock abrasivity classification, University of  
32 Tehran abrasivity test, Wear.

## Abbreviations and their definitions used in this study

Abbreviation	Definition
AV	Abrasion Value
AVS	Abrasion Value Cutter Steel
CAI	Cerchar Abrasivity Index
CCS	Constant Cross Section
$d_u$	Ultimate tip width
$d_f$	First round tip width
DWI	Disc Wear Index
EQC	Equivalent Quartz Content
h	Indentation depth in Rockwell hardness test
HRC	Hardness Rockwell C
HRB	Hardness Rockwell B
LAC	LCPC Abrasivity Coefficient
LCPC	Laboratoire Central Des Ponts Et Chaussées
M	Mass
m	Mass
MEL-TMU	Mechanized Excavation Laboratory of Tarbiat Modares University
NAT	New Abrasion Test
NTNU	Norwegian University of Science And Technology
rpm	round per minute
RIAT	Rolling Indentation Abrasion Test
R-P	Roxborough And Phillips
Scwl	Specific cutter weight loss
SSLCM	Small-Scale Linear Cutting Machine
TBM	Tunnel Boring Machine
UAI	Ultimate Abrasivity Index
UCS	Uniaxial Compressive Strength
UTAI	University Of Tehran Abrasivity Index
UTAT	University Of Tehran Abrasivity Test
$V_{\text{rolling}}$	Rolling velocity
W	Wear Weight

## 39 1. Introduction

40 TBM tunneling has several advantages compared to conventional methods in hard rocks and soft  
41 grounds. Some of those privileges are the higher safety, operating in different geological  
42 conditions, higher advance rate, less disturbance of the surrounding ground, and smooth walls of  
43 the tunnel perimeter (Maidl et al., 2001). Despite the numerous benefits of the mechanized  
44 tunneling, some factors including wear of the cutting tools have adverse impact on the feasibility  
45 of this method, mainly in hard rocks. Therefore, one of the great challenges in hard rock  
46 mechanized tunneling is the wear assessment of the cutting tool, especially disc cutters (Bruland,  
47 1998). The accuracy of the wear prediction models directly affects the costs and duration of  
48 tunneling projects.

49 To address the need for the wear estimation models and in the absence of a standard testing  
50 procedure, several methods have been introduced and utilized for wear evaluation (Gehring, 1995).  
51 Table 1 provides a list of the five common testing methods of estimating the abrasion of materials  
52 and Fig. 1 presents an illustration for these methods. Some of these methods present a qualitative  
53 assessment of the hardness and abrasion of the materials, like the Moh's hardness scale (Paez,  
54 2014), while others provide a quantitative evaluation, such as Cerchar abrasivity test (Alber et al.,  
55 2013).

56 Among the testing methods mentioned in Table 1 that provide a quantitative estimation of wear,  
57 Cerchar and NTNU have some specific strength. For instance, Cerchar abrasivity test has become  
58 one of the most common tests because of the simplicity of its procedure, low cost, fast preparation  
59 of the rock samples, and being susceptible to the main parameters affecting wear including uniaxial  
60 compressive strength (UCS) and equivalent quartz content (EQC), as noted by Rostami et al.  
61 (2014). NTNU test, evaluates the abrasion of the materials based on hardness and resistance of the  
62 rock powder particles (Dahl et al., 2012). This method has a big database and offers a chart to  
63 predict the cutter life, which makes the process of estimating the cutter life much faster and easier  
64 (Dahl et al., 2012).

65 However, conventional abrasivity tests listed in Table 1 have some shortcomings as follows.  
66 Despite the worldwide use of Cerchar test, the results for the same rock samples may vary  
67 significantly. This can be due to several reasons including the absence of a unique standard test  
68 procedure, the type of the device used for the test, pin hardness, roughness of the surface of the  
69 rock sample, and the method used to measure the tip width of the pin (Rostami et al., 2014). As  
70 NTNU test has shown different results for the same samples that were tested in different  
71 laboratories, it is recommended to perform the tests at SINTEF laboratory in order to obtain valid  
72 results (Farrokh and Kim, 2018).

73 LCPC test has smaller database compared to Cerchar and NTNU and also the validity of its results  
74 to be used in estimating the disc cutter wear is along with uncertainties because of the wear  
75 mechanism happens during the test as a result of very fast rotation of the propeller (Farrokh and  
76 Kim, 2018). Assessment of the wear of cutting tools by Rockwell hardness scale has some

77 deficiencies such as small database and not being sensitive to the main parameters affecting the  
78 wear. Moh's hardness scale is also so simple, qualitative, and unable to present an accurate  
79 estimation of abrasion.

80 Beside these deficiencies in conventional abrasivity tests, the design of none of the aforementioned  
81 tests is capable enough to investigate the effect of all aspects of a tribology system. The tribology  
82 system of the rock cutting process consists of the mechanical behavior of the rock and the disc  
83 cutter, and the interaction properties between these two (Hamzaban et al., 2013). In the most  
84 common abrasivity tests, either just the mechanical properties of the rock is studied (e.g. Moh's  
85 and Rockwell hardness scales), or the mechanical behavior of the rock and the disc cutter is  
86 investigated (e.g. Cerchar and NTNU tests), but the influence of the interaction between the disc  
87 and rock is ignored. This interaction is defined as the rolling and indentation mechanism of the  
88 rock cutting process and plays an important role in wear evaluation.

89 In recent years, in order to include the effect of rolling and indentation mechanism on wear,  
90 researchers have introduced several tests which utilize scaled down disc cutters (Farrokh and Kim,  
91 2018; Macias et al., 2016; Sun et al., 2019; Zhang et al., 2018). Some recently developed abrasivity  
92 tests are listed in Table 2 and illustrated in Fig. 2. The main advantage of the recently developed  
93 abrasivity tests, which was completely disregarded in the conventional tests, is their capability to  
94 model the rolling contact between the rock and the disc cutter. Apart from using disc cutters, some  
95 features make them equally feasible tests as conventional approaches. These include using intact  
96 rock, requiring small sample preparation, and utilizing small to medium-sized rock samples.

97 Development of the numerical simulations has motivated researchers to present a model of  
98 estimating wear using finite element and distinct element methods (Galeshi et al., 2020; Xue et al.,  
99 2020). Although using the numerical simulations provides a fast and economical estimation,  
100 experimental approach is believed to be more realistic and acceptable all over the world.

101 In this study, a new method, namely University of Tehran abrasivity test (UTAT), is introduced to  
102 evaluate rock abrasivity using a scaled down V-shaped disc cutter. The method is originally  
103 designed to cover the main drawback of the conventional methods which is ignoring the rolling –  
104 indentation mechanism of the rock cutting process. In this way, the V-shaped disc penetrates the  
105 rock in a preset penetration depth and has its own free rolling motion while moves forward to cut  
106 the surface of the rock. Since this disc cutter is constructed from the same type of steel with  
107 equivalent hardness as the actual-scale disc cutters used in TBM tunneling projects, the proposed  
108 method constitutes a full tribology system.

109

110

111

112

113

**Table 1.** Most common rock abrasivity tests

Test	Procedure	Wear criterion	Correlations	Reference
Cerchar	Scratching the material by a 55 HRC conical pin with 70 N normal force for 10 mm length	Tip width (mm) of the worn conical pin known as the Cerchar Abrasivity Index (CAI)	$CAI = 10 d$	<a href="#">Alber et al., 2013</a>
NTNU	Pushing the test piece on the rock powder (size < 1 mm) with 10 kg normal dead load for 1 to 5 minutes	Weight loss (mg) of the Tungsten or steel test piece known as Abrasion value (AV) or Abrasion Value cutter steel (AVS)	$AV \text{ or } AVS = M_{\text{After}} - M_{\text{Before}}$	<a href="#">Dahl et al., 2012</a>
LCPC	Rotation of a 60-75 HRB rectangular steel impeller for 5 minutes with 4500 rpm rotational speed in a container full of the material powder	Mass loss (g) of the impeller divided by the mass of the sample material (ton) known as LCPC Abrasivity Coefficient (LAC)	$LAC = (m_{\text{after}} - m_{\text{before}}) / M_{\text{material}}$	<a href="#">Thuro et al., 2007</a>
Rockwell hardness	Indentation of a particular indenter into the material	Difference of the indentation depth (mm) at two specific times during the test known as Rockwell C Hardness (HRC)	$HRC = 100 - (h / 0.002)$	<a href="#">Broz et al., 2006</a>
Moh's hardness scale	Scratching the material surface by the specified hardness minerals	Detectable trace of the groove on the softer material	A table of comparative hardness scale of ten selected minerals from Talc to Diamond	<a href="#">Tabor, 1954</a>

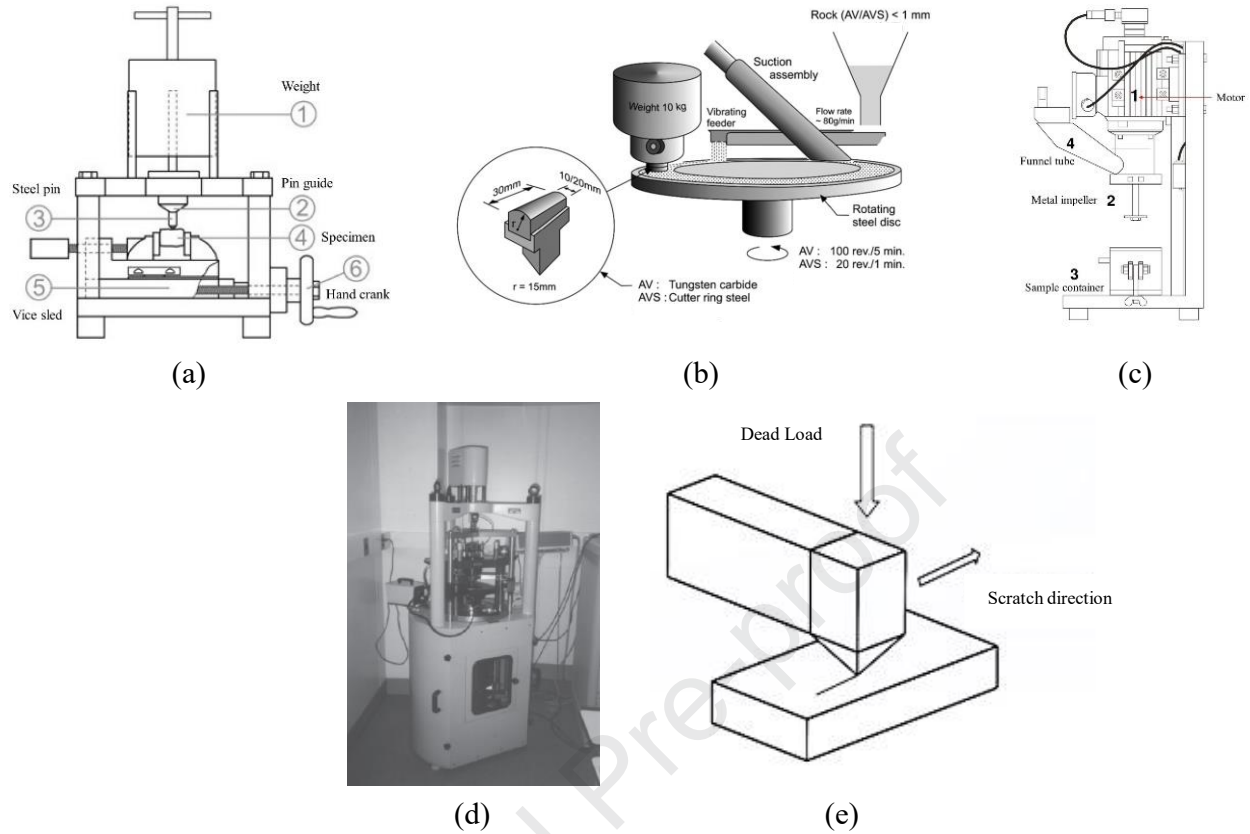
114

115

116

117

118



119

120 **Fig. 1.** The most common abrasion tests (a) Cerchar (Alber et al., 2013) (b) NTNU (Dahl et al.,  
 121 2012) (c) LCPC (Thuro et al., 2007) (d) Rockwell hardness test (Broz et al., 2006) (e) Moh's  
 122 hardness test (Tabor, 1954)

123

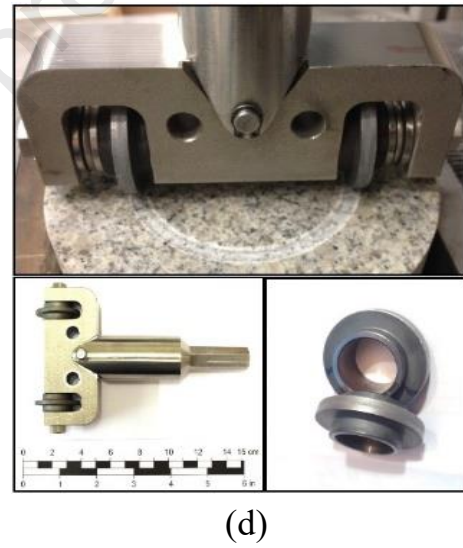
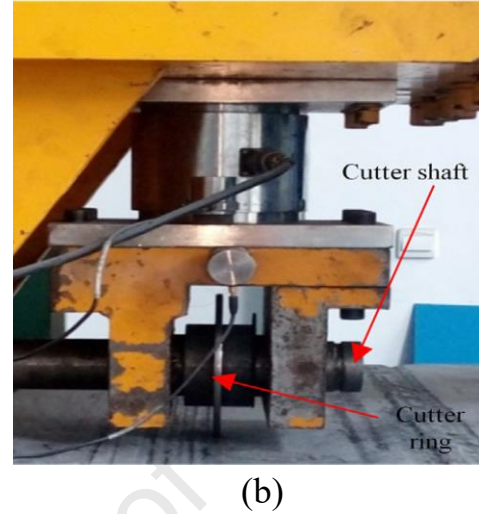
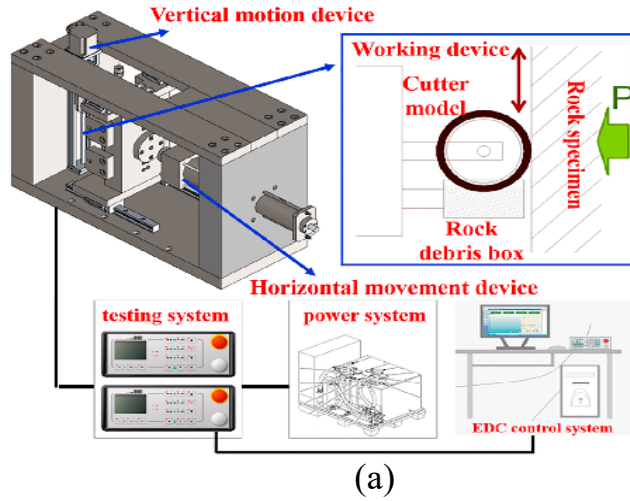
124

**Table 2.** Recently developed abrasivity tests using scaled down disc cutters

Test	Disc features	Disc motion	Disc wear criterion	Correlations	Reference
Composite wear	Hardness 58 HRC Diameter 43.2 mm Thickness 1.9 mm	Penetration 5 mm Distance 100 m	Weight loss (mg) per 100 m of cutting test	$W = 0.7845 CAI^2$	<a href="#">Sun et al., 2019</a>
Central South University of China	Hardness 55-58 HRC Diameter 140 mm Thickness 5 mm	Penetration 1 mm Distance 800 mm $V_{rolling}$ 20 rpm	Weight loss (g)	Graphs of the effect of different disc hardness values on weight loss of the disc	<a href="#">Zhang et al., 2018</a>
New Abrasion Test (NAT)	Hardness 56 HRC Diameter 47 mm Thickness 2 mm	Normal load 25 kg Distance 7.5 m	Specific cutter weight loss (mg/m)	$Scwl = 6.7018 DWI^{0.43}$	<a href="#">Farrokh and Kim, 2018</a>
Rolling Indentation Abrasion Test (RIAT)	Hardness 50 HRC Diameter 30 mm Thickness 4 mm	Normal load 1250 N $V_{Rolling}$ 40 rpm	Weight loss (mg)	$RIAT_a = 2.76 CAI^{1.93}$ $RIAT_a = 4.19 \exp(0.07 AVS)$ $RIAT_a = 2.46 \exp(3.81 EQC)$	<a href="#">Macias et al., 2016</a>

125

126



127

128 **Fig. 2.** Recently developed abrasion tests (a) Composite wear (Sun et al., 2019) (b) Central South  
 129 University of China abrasivity (Zhang et al., 2018) (c) New abrasion (Farrokh and Kim, 2018)  
 130 (d) RIAT (Macias et al., 2016)

131 This system mirrors the mechanical characteristics of both the rock and the cutting tool, as well as  
 132 their rolling-indentation interaction mechanism. A notable feature of this method is the free rolling  
 133 movement of the disc during the cutting operation, which facilitates a smooth and uniform wear  
 134 of the disc tip. Additionally, by limiting the penetration depth, the likelihood of tip damage is  
 135 significantly reduced, allowing for focused examination solely on normal wear patterns.  
 136 Furthermore, by adopting conventional monitoring techniques to this test by measuring the tip  
 137 width, normal wear is differentiated from deformation of the disc. This is an important advantage  
 138 of the monitoring method of this study compared to recently developed abrasivity tests, mentioned  
 139 in Table 2, in which the weight loss of the discs represents the wear and is unable to detect



140 deformation of the tip. The V-shaped design of the discs enables them to penetrate the surface of  
141 rocks with lower force requirements compared to discs with constant cross sections. This design  
142 feature allows for the utilization of testing equipment with lower loading capacities, which are  
143 widely accessible globally. To enhance the applicability of the abrasivity test outputs, two  
144 abrasivity indices are introduced. These indices represent the wear as the function of the  
145 accumulated test run, which makes it possible to classify the abrasion of different rocks.

## 146 **2. Techniques and Facilities**

147 The abrasivity test procedure consists of two steps. First, rock cutting test by a small-scale linear  
148 cutting machine for one round, i.e. cutting length equal to the perimeter of the discs (Section 2.1).  
149 At this point, the tip width of the worn disc is measured using a binocular (Section 2.4). Second,  
150 the rock cutting test continues for a longer cutting length on the worn disc using UTAT machine  
151 (Section 2.2). The tip width is measured sequentially by the binocular after one or several rounds  
152 of the cutting tests. The final cutting length is varied depending on the trend of the measured wear.  
153 All tests are performed at normal room temperature of 20°C. The abovementioned devices are  
154 introduced in the following.

### 155 **2.1 Linear Cutting Machine**

156 The small-scale linear cutting machine (SSLCM) at Mechanized Excavation Laboratory of Tarbiat  
157 Modares University (MEL-TMU) was used for the first round of all abrasivity tests. In other words,  
158 SSLCM was utilized to perform the rock cutting tests using the sharp discs in a distance equal to  
159 their perimeter, which is 170 and 226 mm straight line of cut for the 54 and 72 mm discs,  
160 respectively. Fig. 3 shows the SSLCM which is incorporated for this study. This device consists  
161 of a modified hydraulic shaping machine with 5.9 kW power and maximum ram stroke of 900  
162 mm, dynamometer, cutting tool and rock sample holders, and a data acquisition system  
163 (Mohammadi et al., 2020). Since its development, SSLCM has been fitted with three common  
164 rock cutting tools including chisels, conical picks, and mini-discs (Rostami et al., 2020;  
165 Mohammadi, 2020; Atarian, 2020; Izadshenass, 2019) Cutting velocity and depth are adjustable  
166 but they are fixed on 5 cm/s and 1 mm for all tests. Since this device is capable of monitoring  
167 forces in three directions, it is possible to validate the resulted forces with the theoretical model of  
168 Roxborough and Phillips (1975).

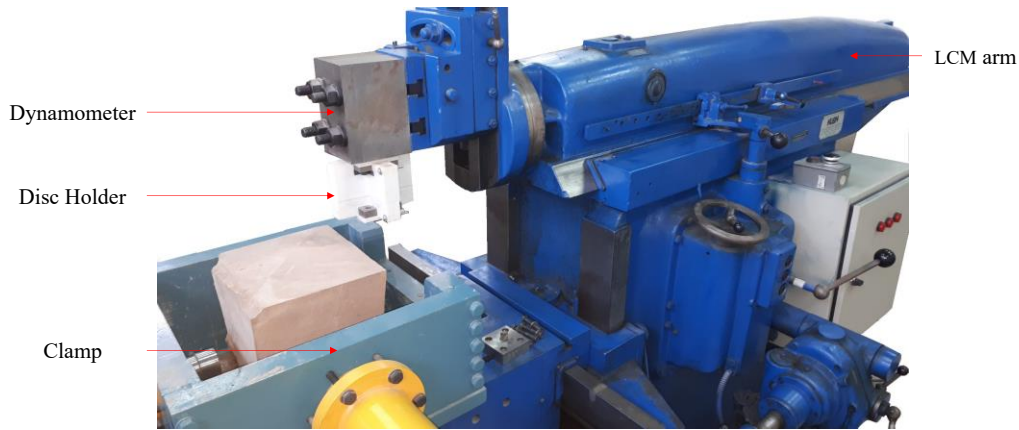


Fig. 3. Small-scale linear cutting machine in MEL-TMU

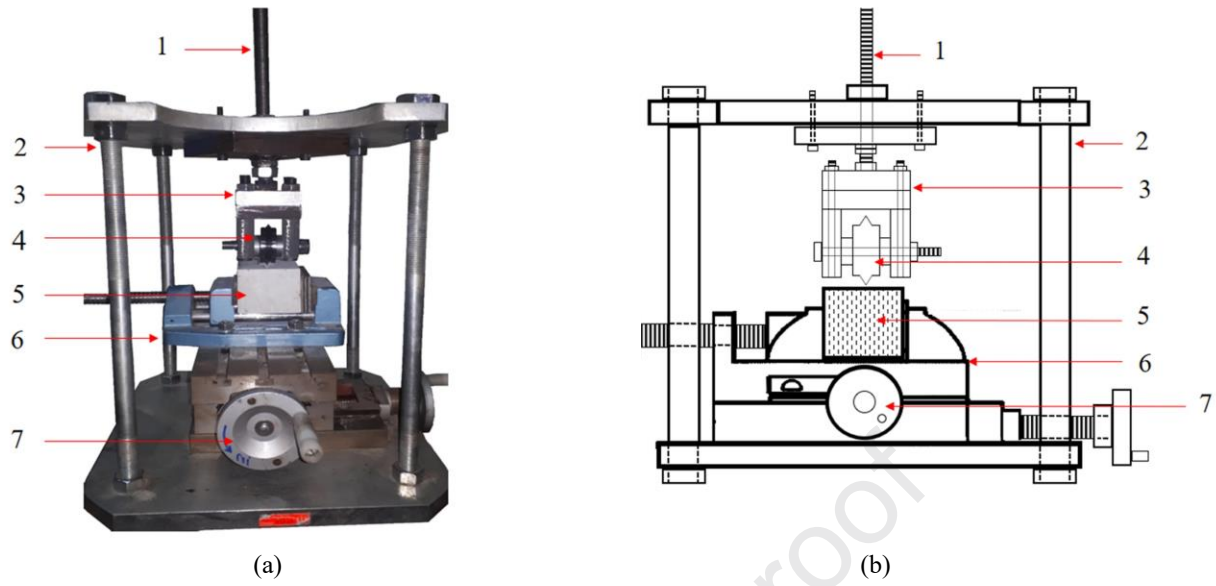
169

170

## 171 2.2 University of Tehran abrasivity test machine

172 After performing the first round of rock cutting, the tip width of the discs were measured by a  
 173 binocular (section 2.4). Then, the second round is done using a new small-scale abrasivity test  
 174 device developed at Rock Mechanics Laboratory of University of Tehran, namely UTAT machine.  
 175 This device consists of a steel frame, disc holder, and a clamp (Fig. 4). Penetration depth is  
 176 adjustable using a screw rod attached to the disc holder while the spacing of the cuts is set by  
 177 positioning the rock sample holder. Regarding the results of the first and second rounds of the  
 178 abrasivity tests, the cutting distance of the third to final round of tests are determined and the tip  
 179 width is measured after the specified cutting distance. Cutting traces by the 54 mm disc with  $80^\circ$   
 180 tip angle on a Basalt sample is shown in Fig. 5. The idea of using a scaled down disc cutter in  
 181 UTAT machine, which is a modified Cerchar apparatus, comes from the similar process that was  
 182 previously utilized in SSLCM and rock cutting tests with miniature discs (i.e. 1 to 2 inches in  
 183 diameter).

184



185

186

187

188

**Fig. 4.** UTAT machine (a) 3D view (b) schematic view (1) Screw rod (2) Steel frame (3) Disc holder (4) Disc (5) Rock sample (6) Clamp (7) Pulley

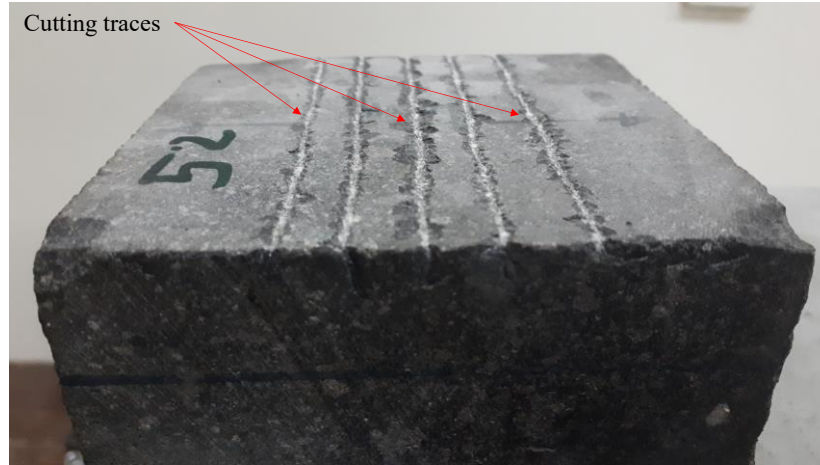


Fig. 5. Cutting traces on a basalt sample

### 2.3 Scaled down disc cutters

Disc cutters are categorized into the V-shaped and the CCS ones based on the cross section shape of the ring. Nowadays, CCS discs with 483 and 432 mm diameter (17" and 19") are the common types due to their higher loading capacity (Rostami, 2008). On the other hand, the V-shaped discs penetrate the rock with lower normal forces because of their sharp tips but the wear rate of this type is much higher (Balci and Tumac, 2012). Since the loading capacity of both abrasivity testing devices used in this investigation is limited and also the wear of the scaled down discs must be detectable, the V-shaped discs were selected for the rock cutting tests. Therefore, four scaled down disc cutters using H13 steel were made, including two 54 mm diameter discs (1/8 scale comparing to the 17" discs) and hardness equal to 54 HRC and the other two 72 mm diameter discs (1/6 scale comparing to the 17" discs) and hardness equal to 32 HRC. The design, geometry and the mechanical properties of the discs are presented in Fig. 6, Table 3 and 4, respectively.

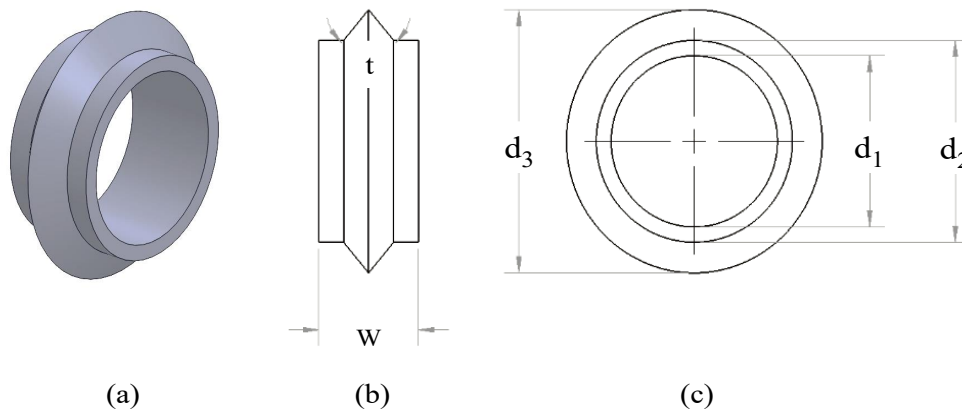


Fig. 6. Schematic views of the disc (a) 3D (b) Side (c) Front

206

**Table 3.** Geometry of the scaled down discs

Disc number	d <sub>1</sub> (mm)	d <sub>2</sub> (mm)	d <sub>3</sub> (mm)	W (mm)	t (deg)
1	35	41	54	22	80
2	35	41	54	22	90
3	35	53	72	22	80
4	35	53	72	22	90

207

208

209

**Table 4.** Mechanical properties of the discs

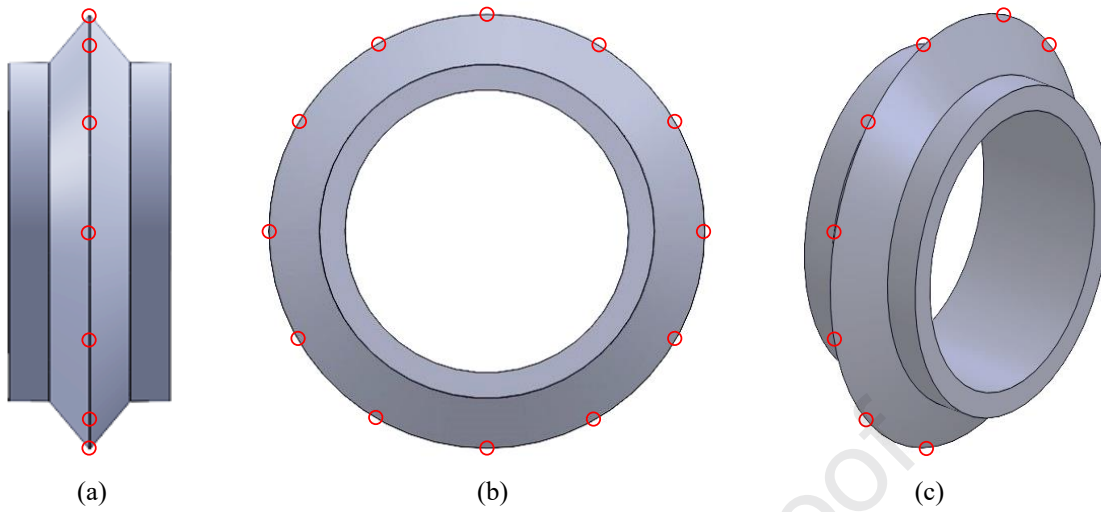
Disc number	Density (kg/m <sup>3</sup> )	Hardness (HRC)	Young's modulus (GPa)	Yield strength (MPa)	Ultimate strength (MPa)
1	7800	54	215	1000	1200
2	7800	54	215	1000	1200
3	7800	32	170	800	1050
4	7800	32	170	800	1050

210

## 211 2.4 Measurement

212 The tip width of each 30 degrees on the perimeter of the disc (total 12 points as shown in Fig. 7)  
 213 is measured both before and after running the cutting tests on the sharp and worn discs,  
 214 respectively. Accordingly, the average of these 12 measurements are reported as the abrasivity test  
 215 results. The measurements are done by a binocular using its maximum magnification (32x) as  
 216 shown in Fig. 8. A digital camera is attached to the binocular to take the pictures of the disc tip.  
 217 For measuring the tip width, discs are fixed vertically above the lower light source of the binocular  
 218 set. This method of analyzing the tip width of the disc captures a section of the disc perimeter (Fig.  
 219 9) which has a quite similar shape comparing to the worn Cerchar pin when the pin is analyzed  
 220 using the method proposed by Rostami et al. (2005). A picture of the worn disc tip from the 54  
 221 mm disc after performing the tests on Basalt is presented in Fig. 9 c.

222



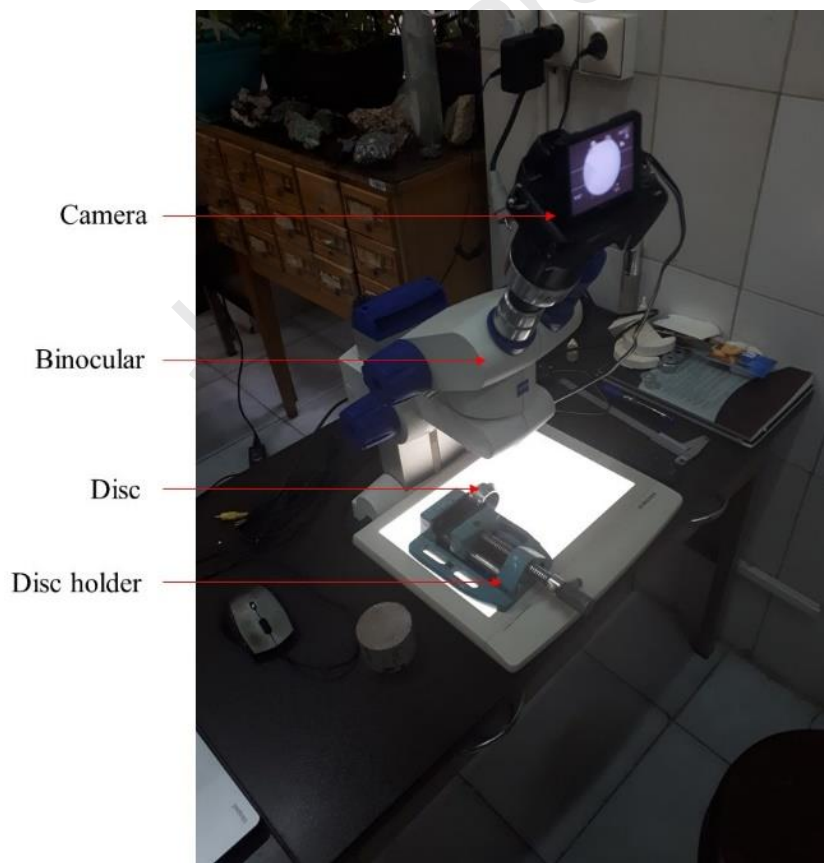
223

224

225

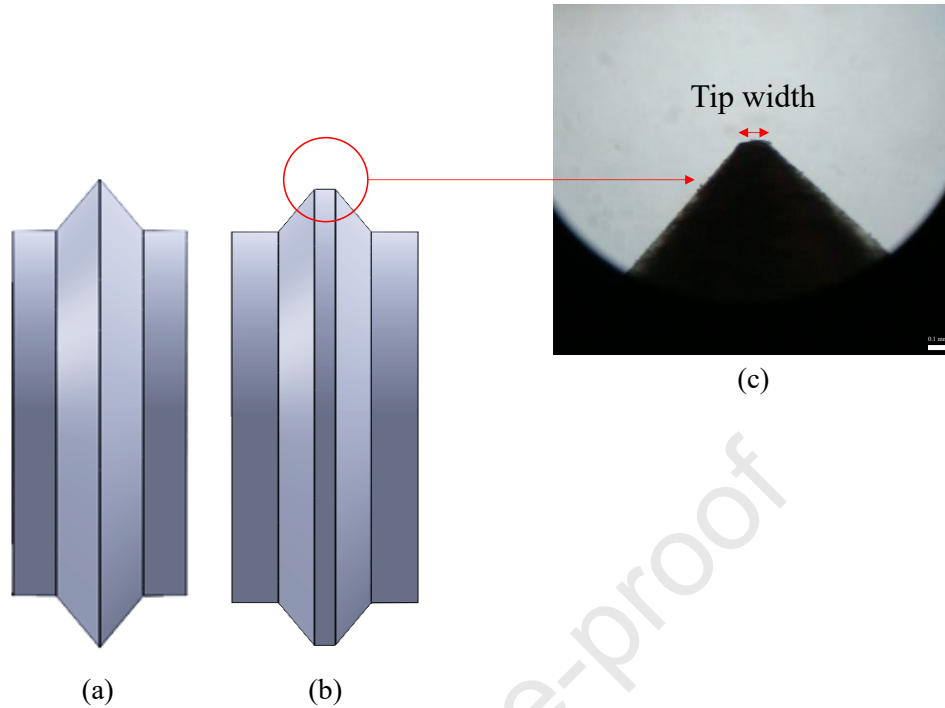
226

**Fig. 7.** Selected points on the disc perimeter for tip width measurement (a) Side view (b) Front view (c) 3D view



227

**Fig. 8.** Binocular and the attached camera for measuring the disc tip width



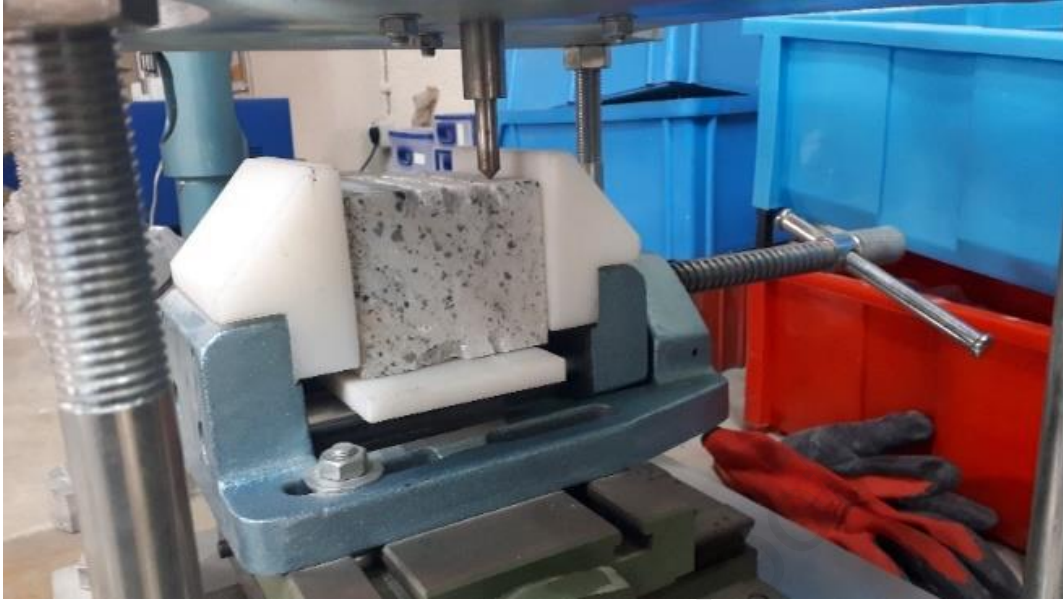
228 **Fig. 9.** Tip width measurement (a) Sharp disc (b) Worn disc (c) Magnified worn tip

## 229 2.5 Sample preparation

230 Three types of rocks are selected including Basalt, Tufa, and Marble. The mechanical properties  
 231 of the rock samples are listed in the Table 3. The range of the UCS for the selected rock types is  
 232 from 62 MPa for Marble to 123 MPa for Basalt that is a wide enough to cover the rocks with  
 233 medium to high UCS based on Deere and Miller (1996) strength classification of intact rocks. All  
 234 of the rock samples are cut and sawn in 10 cm × 10 cm × 15 cm dimensions. Cerchar abrasivity  
 235 tests were also performed three times on each of the rock samples at normal room temperature of  
 236 20°C (Fig. 10). The average of the three results is presented in Table 5.

237 **Table 5.** Mechanical properties of the three rock samples

Rock type	UCS (MPa)	Poisson's ratio	Young's modulus (GPa)	$\phi$ (deg)	Cohesion (MPa)	CAI
Basalt	123	0.2	65	21	0.8	3.15
Tufa	91	0.24	14	11	4.4	1.63
Marble	62	0.11	63	19	5.1	1.13



238  
239 **Fig. 10.** Cerchar abrasivity test on Marble

240

### 241 **3. Results and discussion**

#### 242 **3.1 Wear monitoring**

243 Currently, two methods are being used to monitor the wear of the cutting tools in rock abrasivity  
244 tests. In the first method, the weight loss of the cutting tool is monitored after performing the test  
245 (Farrokh and Kim, 2018; Macias et al., 2016; Sun et al., 2019; Zhang et al., 2018; Dahl et al.,  
246 2012). In the second method, which is incorporated in Cerchar abrasivity test, the microscopic  
247 change of the cutting tool shape (i.e. tip width of the pin) is recorded and defined as the wear  
248 criterion (Alber et al. 2013). Piazzetta et al. (2018) also applied this method to improve abrasivity  
249 classification of rocks. In their study, microscopic changes in the surface of the Cerchar pin were  
250 investigated using a scanning electron microscope.

251 In this paper, regarding the second method, the measured tip width of the discs are presented as a  
252 function of the accumulated test run for different types of rocks. The main privilege of using this  
253 method of monitoring wear is its capability of identifying the wear regime. This feature is applied  
254 to distinguish the normal wear of the V-shaped disc tip from the possible deformations. As it will  
255 be discussed later when presenting the results of the abrasivity tests on the Basalt samples, only  
256 the monitoring of the changes in the shape of the disc tip, not the weight loss of the disc, is able to  
257 detect the normal wear.

258 Analysis of the monitored data is performed by introducing new abrasivity indices that is a  
259 common approach in rock abrasivity tests. Some of the previously developed abrasivity indices  
260 are listed in tables 1 and 2. As mentioned in Table 1, CAI is defined as the ten times of the tip  
261 width ( $d$ ) of the Cerchar pin where the scratch length is set to 10 mm (Eq. 1):

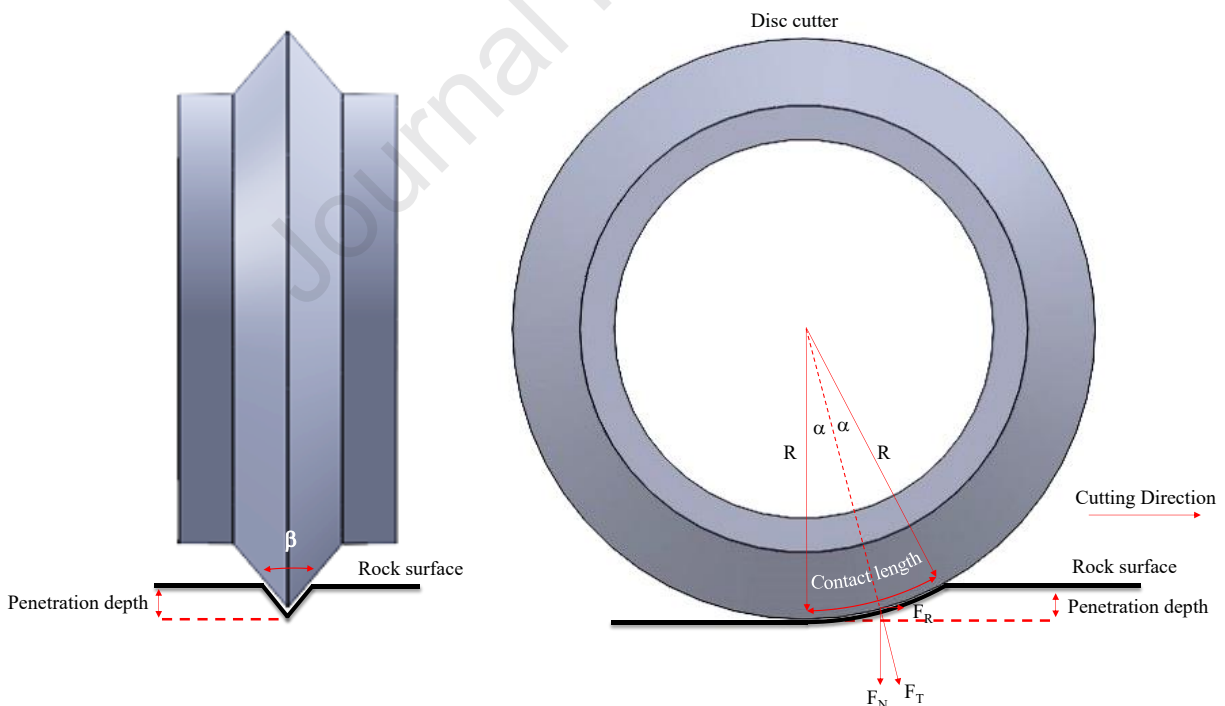


$$262 \quad CAI = 10 d \quad (1)$$

263 In this study, two abrasivity indices are introduced to classify the results. Since the monitoring  
 264 approach used in Cerchar abrasivity test is adopted in this study, the definition of the new  
 265 abrasivity indices follows the same concept. The first index is called the University of Tehran  
 266 abrasivity Index (UTAI) which is defined as the ten times of the measured tip width ( $d_f$ ) after  
 267 performing the first round of the tests (Eq. 2). Regarding the Cerchar abrasivity index shows the  
 268 tip width of the Cerchar pin when the sharp pin is worn after scratching the surface of the rock in  
 269 a predetermined displacement (Alber et al., 2013), UTAI has a similar concept. According to its  
 270 definition (Eq. 2), UTAI represents the tip width of the worn disc when the sharp disc has cut the  
 271 rock in a cutting length equal to its perimeter, i.e. 170 and 226 mm for the discs with 54 and 72  
 272 mm diameter, respectively.

$$273 \quad UTAI = 10 d_f \quad (2)$$

274 This cutting length is set for the abrasivity tests to have the sharp disc equally engaged with the  
 275 rock across its perimeter and therefore, equally worn. The penetration depth of 1 mm is chosen to  
 276 prevent any damage to the disc tip instead of normal wear. At this penetration depth, every point  
 277 on the perimeter of the 54 and 72 mm discs has a contact length of 7.3 and 8.4 mm in each rotation  
 278 of the disc (Fig. 11).



279

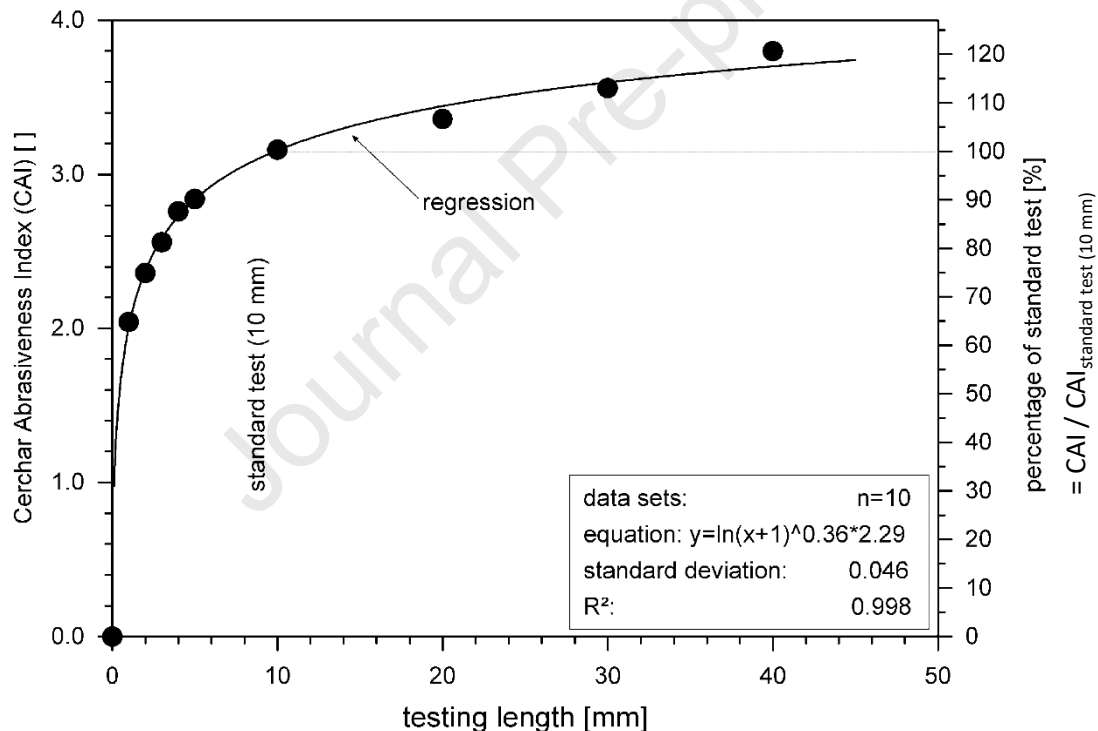
280

**Fig. 11.** Geometry of the rock cutting process

281 The second index is called the Ultimate Abrasivity Index (UAI) which is defined as the ten times  
 282 of the measured tip width ( $d_u$ ) at which the slope of the wear curve, shown in Fig. 13 and 14, has  
 283 started to be horizontal (Eq. 3).

$$284 \quad \text{UAI} = 10 d_u \quad (3)$$

285 The concept of this index displays the effect of the rolling length on the results of the abrasivity  
 286 tests. According to the findings of Al-Ameen and Waller (1994) and Plinninger et al. (2003) about  
 287 the influence of the scratching distance on the results of the Cerchar test, 85 percent of the pin  
 288 wear happens in the first 2 mm of the test (Fig. 12). Then, the wear rate drastically decreases after  
 289 passing 2 mm that in the next 8 mm of the test run, CAI changes just around 15 percent. Fig. 12  
 290 also shows that this drop of the wear rate continuous until 40 mm of the test run, i.e. four times of  
 291 the standard testing length. In this figure, while the left vertical axis shows the CAI at any testing  
 292 length, the right vertical axis represents the percentage of the obtained CAI to the CAI at the  
 293 standard testing length of 10 mm.



294 **Fig. 12.** Plot of CAI versus testing length (Plinninger et al., 2002)

295 A similar trend is observed in the abrasivity tests using scaled down V-shaped discs. According to  
 296 Fig. 13 and 14, the steepest part of the wear curves for each set of the test belongs to their first  
 297 round, in which the disc is worn from its sharpest state. As mentioned earlier, UTAI is introduced  
 298 to represent this part of the wear curves. By continuing the test, a sudden decrease in the wear rate  
 299 is noticeable until the slope of the wear curves has become horizontal. UAI is defined to categorize  
 300 the abrasivity of the rocks based on this point where the cutting tool has undergone the majority

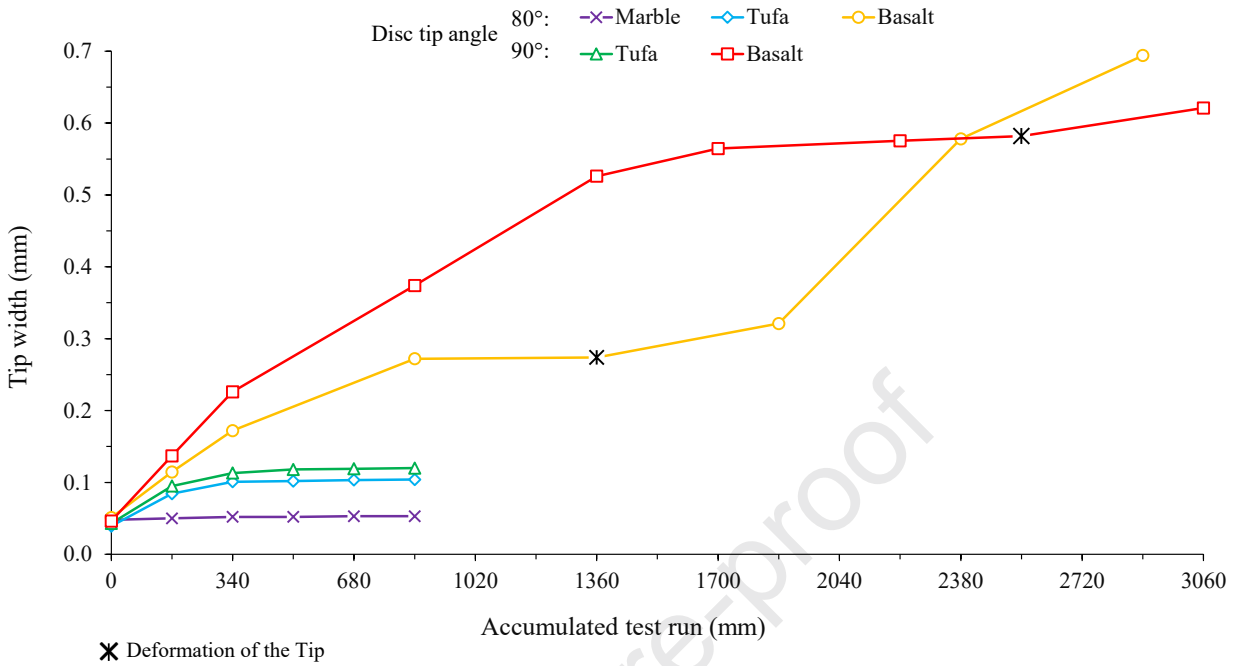
301 of its normal wear. From this point forward, continuing the test will mostly cause deformation of  
302 the tip of the disc with minor normal wear.

303 Fig. 13 shows the wear results of the 54 mm disc with 80° tip angle. Due to the high value of the  
304 disc hardness (54 HRC) and relatively medium UCS of Marble (62 MPa), the disc has remained  
305 almost unworn. The tip width of the disc has been increased from 0.048 to 0.053 mm which shows  
306 only 10 percent change after 5 test run. Abrasivity tests of Tufa show relatively more wear than  
307 Marble that is due to the higher UCS of this rock type. The tip width of the disc has been increased  
308 60 percent after the first round and 100 percent after its ultimate abrasivity value.

309 For Basalt, the wear rate is the highest among all of the first rounds, i.e. 130 percent increase of  
310 the tip width by the first run. This extreme wear continuous until the ultimate abrasivity value is  
311 reached where the tip width has been increased almost 5.5 times. For the next 510 mm running the  
312 test (3 rounds), a negligible wear is measured and the slope of the wear curve is horizontal. Then,  
313 the wear starts again after the 1360 mm test run passes with even higher rate comparing to the first  
314 rounds. The type of wear is different at this time. In the first rounds, normal wear was observed on  
315 the disc tip (Fig. 15 a), while in the last rounds, severe deformation is detectable on the disc tip  
316 (Fig. 15 b).

317

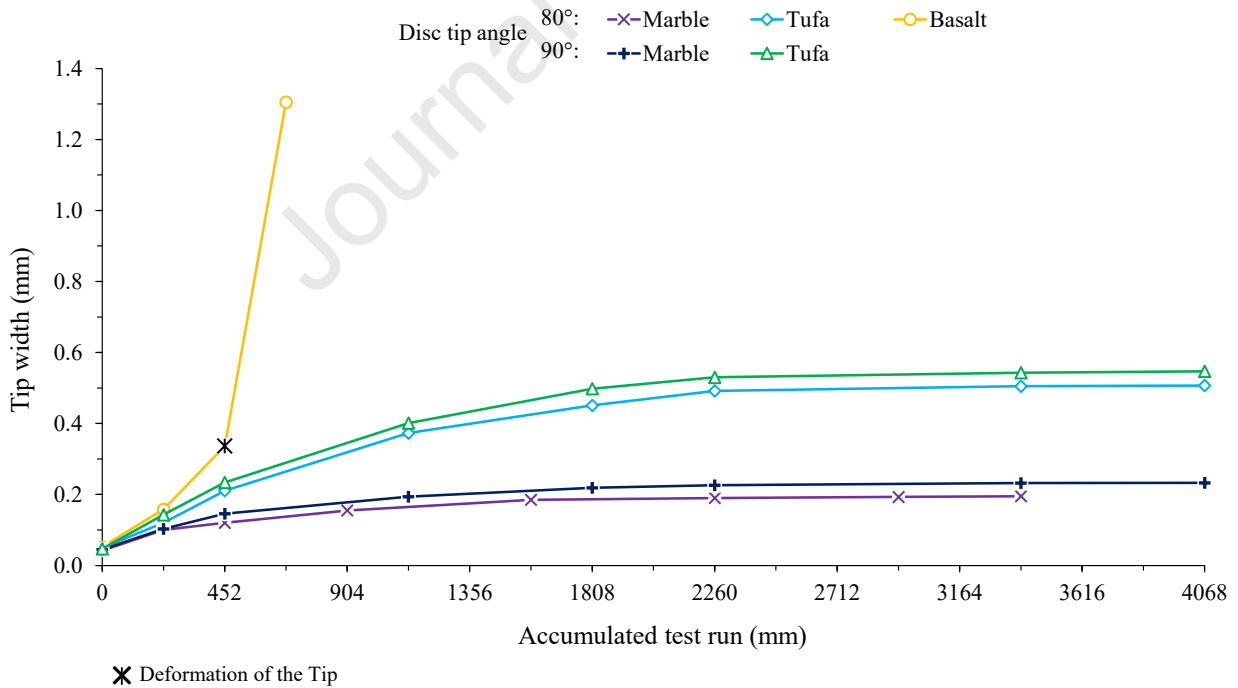
318



319

320

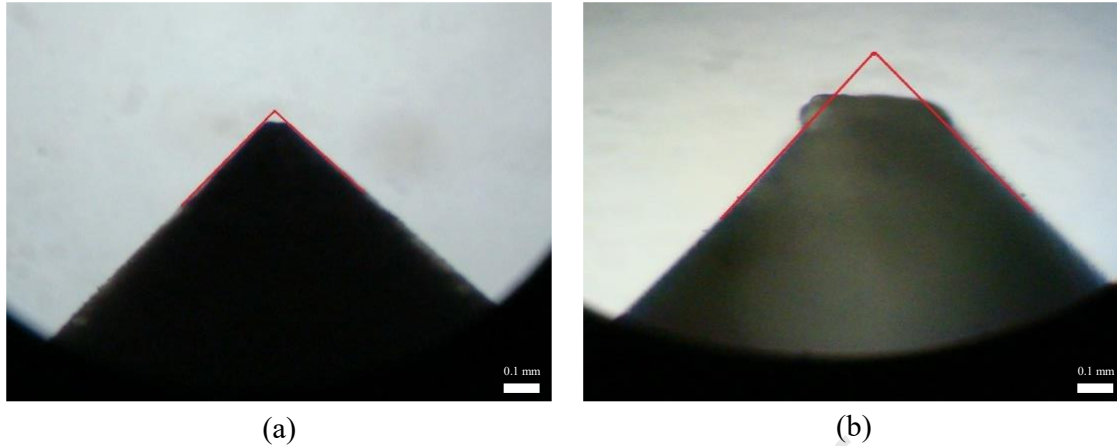
Fig. 13. Wear of the 54 mm discs



321

322

Fig. 14. Wear of the 72 mm discs



323 **Fig. 15.** Types of wear detected on the disc tip (a) Normal wear (b) Deformation

324

325 An explanation for this behavior is that until the 850 mm test run, the cutting forces are not  
 326 adequate to deform the tip. After 1360 mm test run, due to high UCS of Basalt and also bluntness  
 327 of the disc, the disc has experienced higher cutting forces to preserve the 1 mm penetration depth,  
 328 as the penetration depth was set to be constant during the rock cutting process. This extreme  
 329 loading has made some deformations on the disc tip that can be easily seen in Fig. 15 b. The normal  
 330 wear and the deformation of the disc tip can be determined by drawing the lateral lines (the red  
 331 lateral lines) of the disc perimeter. In Fig. 15 b, by drawing the lateral lines, burr is detectable on  
 332 the outside of the line around the disc tip, while in Fig. 15 a, the triangular section of the disc tip  
 333 has just been worn without any deformations. Analysis of the tip deformation is beyond the scope  
 334 of this study.

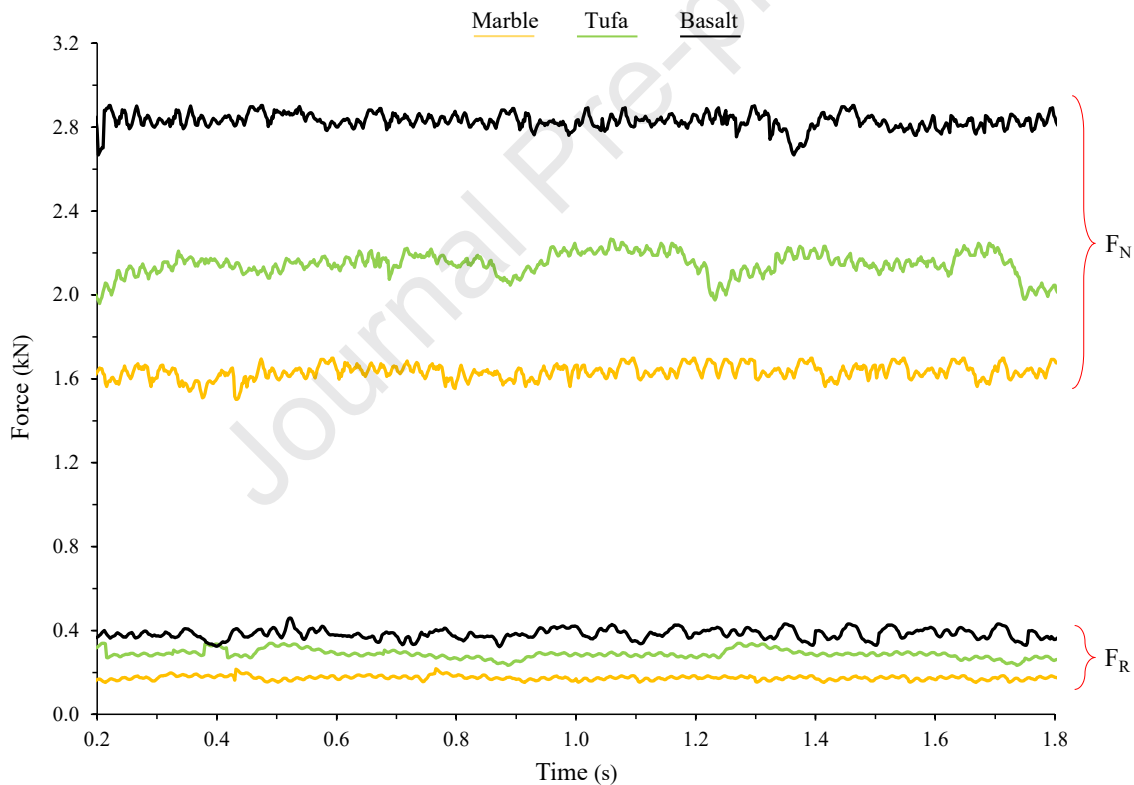
335 Fig. 13 also presents the wear results of the 54 mm disc with  $90^\circ$  tip angle. The results of this set  
 336 of tests show an increase comparing to the  $80^\circ$  tip angle disc. For the Basalt samples, wear rate is  
 337 the highest of the first rounds. Then, the slope of the wear curve becomes horizontal for almost  
 338 510 mm test run (3 rounds) where there is a slight increase of the tip width. It shows that the  
 339 ultimate abrasivity is reached when the tip width is equal to 0.565 mm that is twice the amount of  
 340 UAI comparing to the results on the Basalt samples using the  $80^\circ$  tip angle disc. Meanwhile, in the  
 341 equal test run, i.e. in 850 mm test run, the tip width of the  $90^\circ$  tip angle disc is 0.374 mm which is  
 342 30 percent higher than the UAI of the  $80^\circ$  tip angle disc. The change of the tip angle that results in  
 343 increasing the normal and rolling forces and also modifying the disc shape are some of the reasons  
 344 for this increase of UAI. Wear alongside with deformation restarts after 2550 mm test run with the  
 345 lower ratio comparing to the first rounds, similar to the response of the  $80^\circ$  tip angle disc after  
 346 1360 mm test run.

347 For the Tufa samples, there is a slight increase in the wear results comparing to the previous set of  
 348 the tests but with a similar trend. Since the abrasivity tests on the Marble samples showed almost  
 349 no wear on the  $80^\circ$  tip angle disc cutter, it was expected that it would show the same behavior on  
 350 the  $90^\circ$  tip angle disc. Therefore, no tests were performed on the Marble samples using this disc.

351 Fig. 14 shows the wear results of the 72 mm discs. Lower hardness of these discs (32 HRC) results  
 352 in higher wear for the tests on Marble where the tip width has increased 2.7 and 3.8 times until the  
 353 ultimate abrasivity is reached for the 80° and 90° tip angle discs. The results of the abrasivity tests  
 354 on Tufa and Basalt show an increase in the amount of UTAI and UAI comparing to the 54 HRC  
 355 discs. Although the normal wear was observed in the entire tests on the Tufa samples, an extreme  
 356 deformation happened after the second round on Basalt. The tip width of the disc has been  
 357 increased 3.7 times between the second and third rounds of the test, equal to 225 mm distance.  
 358 This extreme deformation is due to the low hardness of the disc and high UCS of the rock. Since  
 359 studying this extreme deformation was not the subject of this study, no more tests were performed  
 360 on the Basalt samples using 72 mm discs.

### 361 3.2 Cutting forces

362 The normal and rolling forces acting on the discs are monitored using a dynamometer. Fig. 16  
 363 shows an output data of the dynamometer for the 54 mm disc with 80° tip angle.



364

365 **Fig. 16.** Normal and rolling forces on the 54 mm disc with 80° tip angle

366 In this figure, the output forces are presented as the function of the cutting time. In all of the rock  
 367 cutting tests, the 10 cm cut were performed in 2 seconds and the average of the output forces  
 368 between  $t = 0.2$  s and  $t = 0.8$  s were considered as the resulting normal and rolling forces of that  
 369 specific test. The normal and rolling forces graphs of the other discs are almost the same as the

370 Fig. 16, meanwhile in those, the recorded normal and rolling forces oscillate around different levels  
 371 of forces. For example, in Fig. 16, the average normal force acting on the disc 1 for the test on the  
 372 Basalt samples is 2.75 kN, while in the graph for the disc 2, this average value is 3.36 kN.

373 The fluctuation of the forces around an average value is due to the rock cutting process that consist  
 374 of 4 steps (Henneke and Kubler, 1981). At first, the disc touches the surface of the rock and slightly  
 375 penetrates, causing local damage to the rock. At the next step, the disc continues penetrating the  
 376 rock until it reaches the predetermined penetration depth. Then, the normal and rolling forces  
 377 increase until they overcome the UCS of the rock in front of the disc. At the exact moment of the  
 378 rock fragmentation and chipping, those forces reach their highest value and cracks are developed  
 379 to the surface of the rock. At last, the disc rolls forward which results in the drop in the forces. By  
 380 making contact between the rock and the disc again, the aforementioned process repeats.  
 381 Regarding the Fig. 16, this process is so quick and the duration between the two peaks is less than  
 382 20 ms.

### 383 3.3 Abrasivity indices, UCS, and cutting forces

384 Table 6, presents the abrasivity indices, CAI, and the monitored average cutting forces against the  
 385 specifications of the related tests. The plots of the obtained abrasivity indices against the UCS and  
 386 CAI are shown in Fig. 17 a to 17 d. As shown in the Eq. 4 and 5, the following correlations exist  
 387 between UTAI, UAI and UCS for the 54 HRC discs with  $R^2$  of 0.93 and 0.90, respectively:

$$388 \text{UTAI}_{54 \text{ HRC}} = 0.01\text{UCS} - 0.24 \quad (4)$$

$$389 \text{UAI}_{54 \text{ HRC}} = 0.05\exp(0.03\text{UCS}) \quad (5)$$

390 These strong correlations between the abrasivity indices and UCS are observed in the previous  
 391 investigations as well. As mentioned earlier in Table 2, Farrokh and Kim (2018) studied the wear  
 392 of the scaled-down CCS discs. They introduced an abrasivity index called DWI, which represents  
 393 the weight loss of the disc after 7.5 meter of performing the rock abrasivity test, and showed that  
 394 a linear correlation with  $R^2$  of 0.74 exists between DWI and UCS, as presented in Eq. 6:

$$395 \text{DWI} = 1.61\text{UCS} + 100.02 \quad (6)$$

396 By comparing Eq. 4 with Eq. 6, it is obvious that a similar trend exist between UTAI, DWI, and  
 397 UCS, which demonstrates the sensitivity of the tests using disc cutters to the strength properties of  
 398 the rocks and the repeatability of the values obtained as their indices. Eq. 7 and 8 show the  
 399 correlations between UTAI, UAI, and CAI for the 54 HRC discs with  $R^2$  equal to 0.84 and 0.92,  
 400 respectively:

$$401 \text{UTAI}_{54 \text{ HRC}} = 0.32\text{CAI} + 0.28 \quad (7)$$

$$402 \text{UAI}_{54 \text{ HRC}} = 0.41\text{CAI}^{1.96} \quad (8)$$

403 Researchers has studied the wear of the disc cutters and established the relationship between their  
 404 results and other widely used abrasivity indices such as CAI. Sun et al. (2019) studied the wear

405 of CCS discs and proposed a correlation between the wear weight of the disc (W) after 100 m of  
 406 rock cutting test and CAI (Eq. 9):

$$407 \quad W = 0.78CAI^2 \quad (9)$$

408 Comparison of the Eq. 8 with Eq. 9 shows a notable similarity of the relationships between UAI,  
 409 W, and CAI, which verifies the repeatability of the abrasivity tests using disc cutters and the  
 410 applicability of the introduced abrasivity indices. A reason for the similarity of Eq. 4 and 6 between  
 411 the linear relationships of UTAI, DWI and UCS is that both UTAI and DWI are obtained after  
 412 shorter rock cutting length, i.e. UTAI after one round and DWI after 7.5 m of rock cutting tests.  
 413 With the same reasoning, the similarity between the power function of the correlations between  
 414 UAI, W, and CAI in Eq. 8 and 9 is justifiable because UAI and W are defined to represent the  
 415 wear for a longer rock cutting length, i.e. UAI after several rounds and W after 100 m.

416 The average value of the output forces (section 3.2) are also in good agreement with previous  
 417 studies as well. Table 6 presents the average of the cutting forces in this study and estimated values  
 418 from the theoretical Roxborough and Phillips (R-P) model (1975). According to this model, cutting  
 419 forces acting on the V-shaped disc during the rock cutting process is estimated by Eq. 12 and 13:

$$420 \quad F_N = 4\sigma (Dp^3 - p^4)^{1/2} \tan (\beta/2) \quad (10)$$

$$421 \quad F_R = 4\sigma p^2 \tan (\beta/2) \quad (11)$$

422 Where D is the disc diameter, p is the penetration depth, and  $\sigma$  is the UCS of the rock sample. The  
 423 geometry of the rock cutting process is shown in Fig. 11. In this study, since the penetration depth  
 424 is constant in all abrasivity tests, i.e. 1 mm, cutting forces on each disc have linear relationship  
 425 with UCS. As presented in Table 6, comparison of the monitored cutting forces with the R-P model  
 426 shows that the relative error is so small for each set of the rock cutting tests, which verifies the  
 427 abrasivity testing process and the monitored forces.

428 Fig. 17 e and f show the abrasivity indices against the monitored normal forces. Since from the  
 429 theoretical R-P model (Eq. 10 and 11), cutting forces are the functions of UCS and a linear  
 430 correlation is obtained between UTAI and UCS (Eq. 4), a strong relationship is expected between  
 431 the abrasivity indices and cutting forces. However, as the cutting forces depend on the UCS of the  
 432 rocks, the relationships between the abrasivity indices and cutting force are not established in this  
 433 study to avoiding any misleading of presenting the cutting forces as separate variables.

434



435

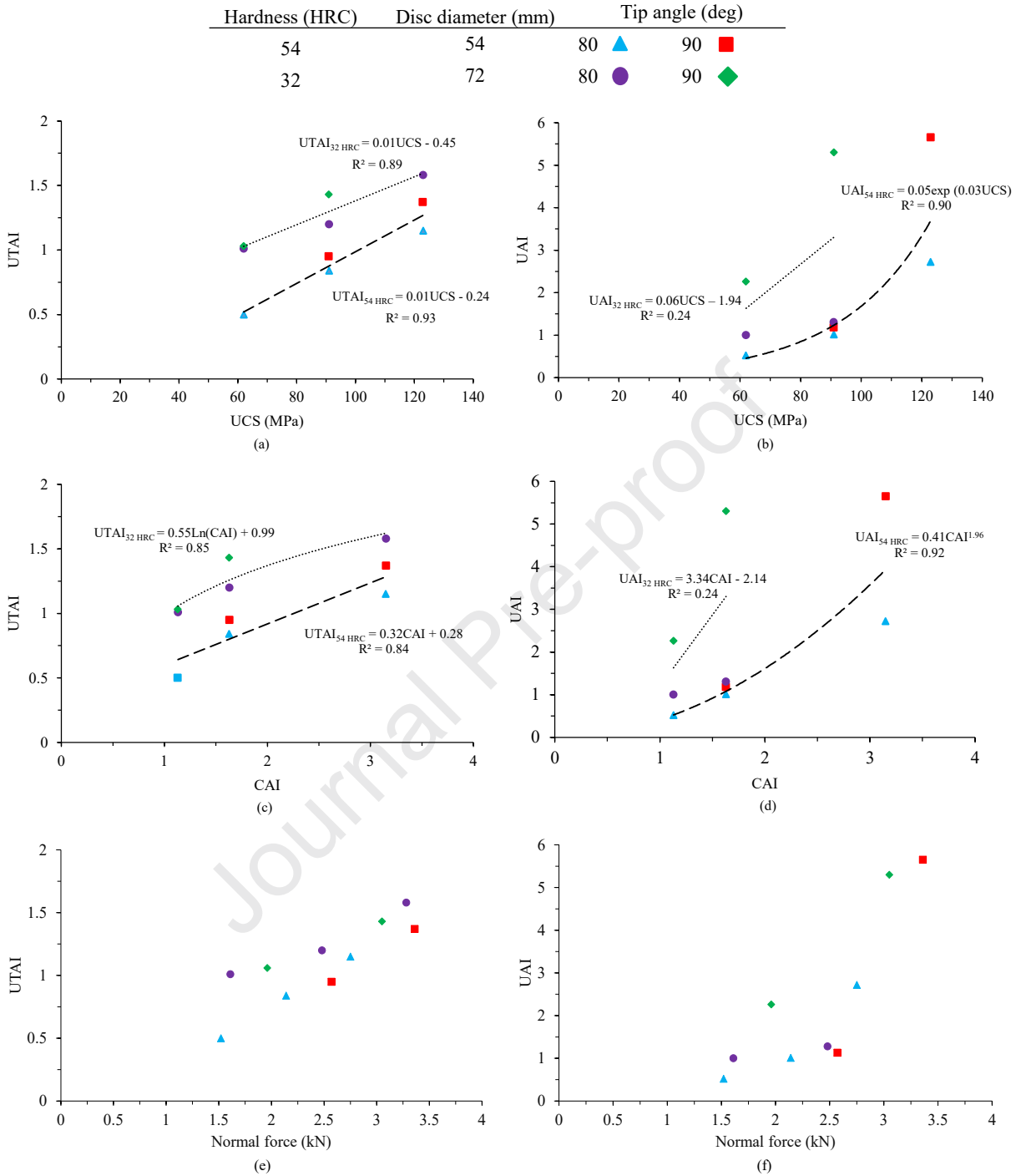
436 **Table 6.** Abrasivity tests results

437

	D (mm)	H* (HRC)	P** (mm)	Tip angle (deg)	UCS (MPa)	CAI (°)	UTAI (°)	UAI (°)	UTAT (kN)		R-P Model (kN)		Relative error (%)	
									F <sub>N</sub>	F <sub>R</sub>	F <sub>N</sub>	F <sub>R</sub>	F <sub>N</sub>	F <sub>R</sub>
Disc 1	54	54	1	80	123	3.15	1.15	2.72	2.75	0.37	2.93	0.4	6.14	7.50
Disc 1	54	54	1	80	91	1.63	0.84	1.01	2.14	0.29	2.20	0.3	2.73	3.33
Disc 1	54	54	1	80	62	1.13	0.5	0.52	1.55	0.19	1.47	0.2	5.44	5.00
Disc 2	54	54	1	90	123	3.15	1.37	5.65	3.36	0.46	3.49	0.48	3.72	4.17
Disc 2	54	54	1	90	91	1.63	0.95	1.18	2.57	0.35	2.62	0.36	1.91	2.78
Disc 2	54	54	1	90	62	1.13	-	-	-	-	1.75	0.24	-	-
Disc 3	72	32	1	80	123	3.15	1.58	-	3.28	0.38	3.39	0.4	3.24	5.00
Disc 3	72	32	1	80	91	1.63	1.2	1.20	2.48	0.31	2.55	0.3	2.75	3.33
Disc 3	72	32	1	80	62	1.13	1.01	1.00	1.61	0.18	1.70	0.2	5.29	10.00
Disc 4	72	32	1	90	123	3.15	-	-	-	-	4.04	0.48	-	-
Disc 4	72	32	1	90	91	1.63	1.43	5.30	3.05	0.32	3.07	0.36	0.65	11.11
Disc 4	72	32	1	90	62	1.13	1.03	2.26	1.96	0.22	2.02	0.24	2.97	8.33

\* Hardness

\*\* Penetration



438 **Fig. 17.** Correlation between the abrasivity tests results (a) UTAI – UCS (b) UAI – UCS (c)  
 439 UTAI – CAI  
 440 (d) UAI – CAI (e) UTAI – Normal force (f) UAI – Normal force

441

442

#### 443 4. Conclusion

444 Estimating the wear of a cutting tool is a great challenge since the performance of the mechanized  
445 tunneling machines directly affects the duration and costs of the projects. University of Tehran  
446 abrasivity test is introduced to estimate the wear of the disc cutters by performing laboratory rock  
447 cutting tests using scaled down discs. In this test, comparing to the Cerchar pin, there is more  
448 similarity between the shape of the cutting tool and real-scale disc cutters and besides, this tool  
449 penetrates the rock while having its free rolling motion. Therefore, the test closely resembles the  
450 rock cutting process and consequently, those parameters that affect the disc wear. The method of  
451 measuring the tip width of the cutting tool, instead of its weight, is utilized in this study that makes  
452 it possible to distinguish the normal wear from the deformations, as it is necessary to differentiate  
453 these types of wear to optimize the performance of the disc cutters before they undergone excessive  
454 deformations. Two abrasivity indices are defined, namely UTAI and UAI, to easily interpret the  
455 relationships between the mechanical properties of the rocks and the abrasivity test results. Each  
456 of these indices has a similar concept comparing to the Cerchar abrasivity index, as UTAI  
457 represents the wear of the sharp cutting tool and UAI displays the effect of the testing length. The  
458 correlations between the abrasivity indices, UCS and CAI are established, which shows strong  
459 relationships between them. This means that the introduces abrasivity test is capable enough to  
460 cover all aspects of the tribology system of a rock cutting procedure using disc cutters. Moreover,  
461 UTAI and UAI are highly sensitive to the mechanical properties of the discs and rock samples,  
462 which makes them good representatives of the disc wear. Comparison of these equations and those  
463 of the previous studies also shows the similarity between them that perfectly demonstrates the  
464 repeatability of the output data of the recently designed abrasivity tests using scaled down disc  
465 cutters. Moreover, the testing process is verified by comparing the monitoring cutting forces with  
466 theoretical model in the previous studies. Since the University of Tehran abrasivity test closely  
467 resembles the rock cutting process using disc cutters, it is able to distinguish between the normal  
468 wear and deformation, and its results are in good agreement with the mechanical properties of  
469 rocks, using this method can enhance the accuracy of the rock abrasivity classifications. Moreover,  
470 some features of this method increase the feasibility of worldwide utilization of this test including  
471 the small sample preparation, fast testing procedure, and simple testing apparatus with low  
472 capacity that is widely accessible.

473

#### 474 CRediT authorship contribution statement

475 **Maziar Moradi:** Conceptualization, Methodology, Formal analysis, Investigation, Data curation,  
476 Writing - original draft. **Mohammad Hossein khosravi:** Methodology, Validation, Resources,  
477 Writing – Review and editing, Supervision, Project administration. **Jafar Khademi Hamidi:**  
478 Methodology, Validation, Resources, Writing – Review and editing, Supervision.

479

480

481 **Declaration of competing interests**

482 The authors declare that there is no conflict of interest regarding the publication of this article  
 483 and they did not receive support from any organization for the submitted work.

484

485 **References**

- 486 Al-Ameen, S.I., Waller, M.D., 1994. The influence of rock strength and abrasive mineral content  
 487 on the Cerchar abrasive index. *Engineering Geology*, 36(3-4), pp.293-301.
- 488 Alber, M., Yarali, O., Dahl, F., Bruland, A., 2013. ISRM suggested method for determining the  
 489 abrasivity of rock by the CERCHAR abrasivity test. *Rock Mechanics and Rock Engineering*.  
 490 10.1007/s00603-013-0518-0.
- 491 Atarian, A., 2020. A laboratory study of the effect of tool geometry on rock cutting efficiency.  
 492 M.Sc. Thesis, Mining Engineering Department, Tarbiat Modares University.
- 493 Balci, C., Tumaç, D., 2012. Investigation into the effects of different rocks on rock cuttability by  
 494 a V-type disc cutter. *Tunnelling and underground space technology*, 30, pp.183-193.
- 495 Broz, M.E., Cook, R.F., Whitney, D.L., 2006. Microhardness, toughness, and modulus of Mohs  
 496 scale minerals. *American Mineralogist*, 91(1), pp.135-142.
- 497 Bruland, A., 1998. Hard Rock Tunnel Boring – Advance Rate and Cutter Wear. Project report 1B-  
 498 98, NTNU.
- 499 Dahl, F., Bruland, A., Jakobsen, P.D., Nilsen, B., Grøv, E., 2012. Classifications of properties  
 500 influencing the drillability of rocks, based on the NTNU/SINTEF test method. *Tunnelling and*  
 501 *Underground Space Technology*, 28, pp.150-158.
- 502 Deere, D.U., Miller, R.P., 1966. Engineering classification and index properties for intact rock,  
 503 Technical Report No. AFNL-TR, Air Force Weapons Laboratory, New Mexico, pp. 65–116.
- 504 Farrokh, E., Kim, D.Y., 2018. A discussion on hard rock TBM cutter wear and cutterhead  
 505 intervention interval length evaluation. *Tunnelling and Underground Space Technology*, 81,  
 506 pp.336-357.
- 507 Galeshi, M.Z., Goshtasbi, K., Hamidi, J.K., Ahangari, K., 2020. A Numerical Investigation of  
 508 TBM Disc Cutter Life Prediction in Hard Rocks. *Journal of Mining and Environment (JME)*,  
 509 11(4), pp.1095-1113.
- 510 Gehring, K.H., 1995. Performance and wear prediction in mechanized tunneling. *Rock*  
 511 *Engineering*, 13, No. 6.
- 512 Hamzaban, M.T., Memarian, H., Rostami, J., 2013. Comparison of various rock abrasivity testing  
 513 methods. *Iranian Journal of Mining Engineering*, 8(19), pp.87-106.
- 514 Henneke, J., kubler, H., 1981. ergebnisse, erfahrungen und entwicklungstendenzen beim einsatz  
 515 von tunnelbohrmaschinen im steinkohlenbergbau, pp.145-192.
- 516 Izadshenass jahromi, M., 2019. Design and fabrication of a disc cutter for use in Small-scale linear  
 517 rock cutting machine (SSLRCM). M.Sc. Thesis, Mining Engineering Department, Tarbiat  
 518 Modares University.
- 519 Macias, F.J., Dahl, F., Bruland, A., 2016. New rock abrasivity test method for tool life assessments  
 520 on hard rock tunnel boring: the rolling indentation abrasion test (RIAT). *Rock Mechanics and*  
 521 *Rock Engineering*, 49(5), pp.1679-1693.
- 522 Maidl, B., Schmid, L., Ritz, W., Herrenknecht, M., 2008. Hardrock tunnel boring machines. John  
 523 Wiley & Sons.

- 524 Mohammadi, M., Khademi Hamidi, J., Rostami, J., Goshtasbi, K., 2020. A Closer Look into Chip  
 525 Shape/Size and Efficiency of Rock Cutting with a Simple Chisel Pick: A Laboratory Scale  
 526 Investigation. *Rock Mech. Rock Eng.* 53, pp. 1375–1392. [https://doi.org/10.1007/s00603-019-](https://doi.org/10.1007/s00603-019-01984-5)  
 527 01984-5.
- 528 Mohammadi, M., 2020. Rock cuttability by drag picks under lateral loading. Ph.D. Thesis, Mining  
 529 Engineering Department, Tarbiat Modares University.
- 530 Paez, C.V.G., 2014. Performance, wear and abrasion in excavation mechanized tunneling in  
 531 heterogeneous land. PhD thesis, Universitat Politècnica de Catalunya (UPC).
- 532 Piazzetta, G.R., Lagoeiro, L.E., Figueira, I.F.R., Rabelo, M.A.G., Pintaude, G., 2018.  
 533 Identification of abrasion regimes based on mechanisms of wear on the steel stylus used in the  
 534 Cerchar abrasiveness test. *Wear*, 410, pp.181-189.
- 535 Plinninger, R., Käsling, H., Thuro, K., Spaun, G., 2003. Testing conditions and geomechanical  
 536 properties influencing the CERCHAR abrasiveness index (CAI) value. *International journal of*  
 537 *rock mechanics and mining sciences*, 40(2), pp.259-263.
- 538 Rostami, J., 2008. Hard Rock TBM Cutterhead Modeling for Design and Performance Prediction.  
 539 *Geomechanik Tunnelbau*, 1: 18-28. <https://doi.org/10.1002/geot.200800002>.
- 540 Rostami, J., Ghasemi, A., Alavi Gharahbagh, E., Dogruoz, C., Dahl, F., 2014. Study of dominant  
 541 factors affecting Cerchar abrasivity index. *Rock mechanics and rock engineering*, 47(5),  
 542 pp.1905-1919.
- 543 Rostami, J., Ozdemir, L., Bruland, A., Dahl, F., 2005. Review of issues related to Cerchar  
 544 abrasivity testing and their implications on geotechnical investigations and cutter cost  
 545 estimates. *Proceedings of the RETC*, pp.738-751.
- 546 Rostami, K., Hamidi, J.K., Nejati, H.R., 2020. Use of rock microscale properties for introducing a  
 547 cuttability index in rock cutting with a chisel pick. *Arabian Journal of Geosciences*, 13(18),  
 548 pp.1-12.
- 549 Roxborough, F.F., Phillips, H.R., 1975. Rock excavation by disc cutter. *International Journal of*  
 550 *Rock Mechanics and Mining Sciences & Geomechanics Abstracts*, Vol. 12, No. 12, pp. 361-  
 551 366.
- 552 Sun, Z., Zhao, H., Hong, K., Chen, K., Zhou, J., Li, F., Zhang, B., Song, F., Yang, Y., He, R.,  
 553 2019. A practical TBM cutter wear prediction model for disc cutter life and rock wear  
 554 ability. *Tunnelling and Underground Space Technology*, 85, pp.92-99.
- 555 Tabor, D., 1954. Mohs's hardness scale-a physical interpretation. *Proceedings of the Physical*  
 556 *Society, Section B*, 67(3), p.249.
- 557 Thuro, K., Kaesling, H., Bauer, M., 2007. Determining abrasivity with the LCPC test. *Proceedings*  
 558 *of the 1st Canada-US Rock Mechanics Symposium - Rock Mechanics Meeting Society's*  
 559 *Challenges and Demands*, 1. 827-834. 10.1201/NOE0415444019-c103.
- 560 Xue, Y., Fan, Y., Li, X., Xu, L., 2020. Study on TBM Disc Cutter Wear Process Based on a New  
 561 DEM Model. In *54th US Rock Mechanics/Geomechanics Symposium*, OnePetro.
- 562 Zhang, X., Lin, L., Xia, Y., Tan, Q., Zhu, Z., Mao, Q., Zhou, M., 2018. Experimental study on  
 563 wear of TBM disc cutter rings with different kinds of hardness. *Tunnelling and Underground*  
 564 *Space Technology*, 82, pp.346-357.

## Highlights

- The proposed method of estimating wear is capable of improving the process of evaluating wear due to the fact that the same mechanism of rock cutting is being used compared to the mechanized tunneling machines. This mechanism is defined as penetrating the rock using the disc and making the cut by rolling the disc while maintaining the penetration depth. Despite the previous methods, like Cerchar test that represents the influence of the mechanical properties of the rock sample and the cutting tool on wear, the new method evaluates wear by being sensitive to all aspects of the tribology system including the wear mechanism, too.
- The presented test procedure is quite fast, simple, with small preparation of the rock samples and discs. The discs are made of H13 steel, which is the same type of steel used in real scale discs, and scaled down to 54 mm and 72 mm diameter, which is 1/8 and 1/6 down scale comparing to the actual disc cutters with 432 mm diameter. The rock samples are selected to cover a wide range of UCS from 62 MPa to 123 MPa in 10 cm × 10 cm × 15 cm dimensions. The small size of the samples is an advantage due to the harder preparation of large samples.
- The results of the new abrasivity tests are in good agreement with previous studies. For instance, by increasing the uniaxial compressive strength and Cerchar abrasivity index of the rock samples, the wear rate has gradually doubled. Besides, monitored data of the normal and rolling forces acting on the discs are so close to theoretical calculations based on Roxborough and Philips model. Moreover, the measurement method has made it possible to differentiate the normal wear with deformation of the discs and new defined abrasivity indices has made it easier and more accurate to compare the test results with each other and classifying rocks based on their abrasivity.

**Declaration of interests**

The authors declare that they have no known competing financial interests or personal relationships that could have appeared to influence the work reported in this paper.

The authors declare the following financial interests/personal relationships which may be considered as potential competing interests:

Journal Pre-proof